# Human-Manipulator Interface Using Hybrid Sensors via CMAC for Dual Robots

P. Zhang, G. Du, B. Liang, X. Wang

**Ping Zhang, Guanglong Du\***
South China University of Technology, China
pzhang@scut.edu.cn, medgl@scut.edu.cn
*Corresponding author: medgl@scut.edu.cn

**Bin Liang, Xueqian Wang**
Graduate School at Shenzhen, Tsinghua University, China
bliang@tsinghua.edu.cn, wang.xq@sz.tsinghua.edu.cn

**Abstract:** This paper presents a novel method that allows a human operator to communicate his motion to dual robot manipulators by performing his double hand-arms movements, which would naturally carry out an object manipulation task. The proposed method uses hybrid sensors to obtain the position and orientation of the human hands. Although the position and the orientation of the human hands can be obtained from the sensors, the measurement errors increase over time due to the noise of the devices and the tracking error. A cerebellar model articulation controller (CMAC) is used to estimate the position and orientation of the human hands. Due to the limitations of the perceptive and the motor, human operator can not accomplish the high precise manipulation without any assistants. An adaptive multi-space transformation (AMT) is employed to assist the operator to improve the accuracy and reliability in determining the posture of the manipulator. With making full use of the human hand-arms motion, the operator would feel kind of immersive. Using this human-robot interface, the object manipulation task done in collaboration by dual robots could be carried out flexibly through preferring the double hand-arms motion by one operator.

**Keywords:** Cerebellar Model Articulation Controller (CMAC), robot teleoperation, human-robot interface.

## 1 Introduction

Human intelligence is required to make a decision and control the robot especially when it is in unstructured dynamic environments. Thus, robot teleoperation is necessary especially when the robot is in highly unstructured environments, where objects are unfamiliar or changing shape. There are some human-robot interfaces which have been commonly used [1], such as dials and robot replicas. However, for completing a teleoperation task, these contacting mechanical devices always require unnatural hand and arm motion.

There is another way to communicate complex motions to a remote robot and it is more natural that comparing with using contacting mechanical devices. This method is to track the operator hand-arm motion which is used to complete the required task using inertial sensors, contacting electromagnetic tracking sensors, gloves instrumented with angle sensors, and exoskeletal systems [2]. However, these contacting devices may hinder natural human-limb motion. Vision-based techniques are non-contacting and they are less hindering the hand-arm motion. Vision-based methods often use physical markers which are placed on the anatomical body part [3]. There are a lot of applications [4] based on marker-based tracking of the human motion. However, because body markers may hinder the motion for some highly dexterous tasks and operators may be occluded, the marker-based tracking is not always practical. Thus, a markerless approach seems better for many applications.

Compared with image-based tracking which uses markers, markerless is not only less invasive, but also can eliminate problems of marker occlusion and identification [5]. Thus, for remote robot teleoperation, markerless tracking may be a better approach. However, the existing markerless human-limb tracking techniques have many limitations so that they may be difficult to use in robot teleoperation applications. Many existing markerless-tracking techniques capture images and then compute the motion later [6, 7]. The robot manipulator could be controlled with the continuous robot motion by the markerless tracking. To allow the human operator to perform hand-arm motions for a task in a natural way without any interruption, the position and orientation of the hand and arm should be provided immediately. Many techniques can only provide 2D image information of the human motion [8], but the tracking methods cannot be extended for accurate 3D joint-position data. An end-effector of a remote robot would require the 3D position and orientation information of the operators limb-joint centers with respect to a fixed reference system. The problem how to identify human body parts in different orientations has always been a main challenge [9].

For robot teleoperation, some limited research towards markerless human-tracking has been done. Many techniques used a human-robot interface based on hand-gesture recognition to control the robot motion. Ionescu et al [10] developed markerless hand-gesture recognition methods which can be used for mobile robot control where only a few different commands are sufficient such as go, stop, left, right. However, for object manipulation in 3D space, it is not possible to achieve natural control and flexible robot motion by using gestures only. If a human operator wants to use gestures, he/she needs to think of those limited separate commands that the human-robot interface can understand like move up, down, forward. A better way of human-robot interaction would permit the operator to focus on the complex global task as a human operator naturally does when grasping and manipulating objects in 3D space instead of thinking about which type of hand motions are required. To achieve this goal, a method that allows the operator to complete the task using the hand-arm motions naturally provides the robot with information of the hand-arm motion in real time, that is the hand and arm anatomical position and orientation [11, 12]. However, method [11] is hard to obtain the accurate orientation of the human hand since the occlusion easily happens. To achieve the initialization, the human operator must assume a simple posture with an unclothed arm in front of a dark background, and the hand should be higher than the shoulder. Therefore, through the method [12], it is not possible to get precise results under a complex background. In addition, the human operator is hard to work in the chill weather with unclothed arm. And also it is limited because of lighting effect, which is difficult to work where the environment is too bright or too dark.

As the manipulation taskbeing more complex, multiple robot cooperation will be a trend. Vision-based methods mentioned above are hard to use in the multi-robot interface, as they can solve the occlusion problem. In addition, the contacting interfaces used in teleoperation for the multiple robot manipulators often require multiple operators [13].

This article presents a method of dual robot-manipulators interface using hybrid sensors to track the hand of the human operator (Fig. 1). Hand tracking based hybrid sensors is used to acquire 3D anatomical position and orientation and sent the data to the robot manipulator by a human-robot interface, which enables the robot end-effector to copy the operator hand motion in real time.

Fig. 2 shows the structure of our system. A position sensor provides the location of the human hand and an IMU provides the orientation of the human hand. We use Camshift to track the human hand. An IMU consisting of gyroscopes and magnetometer can measure the orientation and the acceleration of the hand. A CMAC estimation algorithm is used to estimate the positions and the accelerations of the hand. Another CMAC is applied to estimate the orientation and the angular velocities of the hand. In order to eliminate the influence of the noise and the

tracking failure, speed control method is used instead of the absolute location control method. The velocity value is transmitted to the manipulator and the manipulator moves at the received rate. The velocities of the position and the orientation are processed via AMT to improve the accuracy of manipulation. The natural way to communicate with the robots allows the operator to focus on the task instead of thinking the limited separate commands that the human-robot interface can understand like gesture- based approaches. There may be marker occlusion and identification when using vision-based approaches. In addition, this way let the operator feel kind of immersive in the multi-robot environment, which feels that his hands are in the robot site.

In Section 2, the CMAC method is presented. The human hand tracking system is then detailed in Section 3. Section 4 describes AMT method. Experiments and results are presented in Section 5. Discussions of this paper are detailed in Section 6, followed by concluding remarks in Section 7.
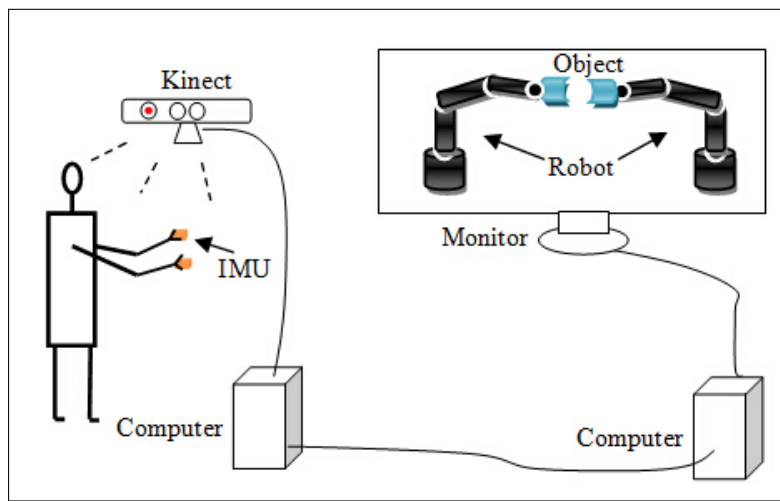


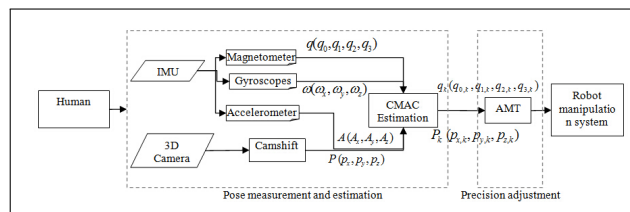Figure 1: Non-invasive robot teleoperation system based on the Kinect



Figure 2: The structure of the system

## 2   Cerebellar Model Articulation Controller (CMAC)

Since the signals of the position and the orientation of human hand are time-varying and they are ill-defined when occlusion is encountered, an adaptive filter is required. In this paper, we use CMAC to process the pose signal (position and orientation). The convergence of CMACoutput error can be guaranteed because the stable conditions of the adaptive learning-rates are derived based on the Lyapunov function [14].

There are five components in CMAC: input space, association memory space, receptive-field space, weight memory space, and output space. The flow of CMAC is as follows:

(1) Input space C: The input vectoris $c = [c_1, c_2, ..., c_n]^T \in R$ according to a given control space. $c_i$ is the input state variable and $n$ is the input dimension. Each input state variable $c_i$ must be quantized into discrete regions (element).

(2) Association memory space A: Several elements can be accumulated as a block B and each block performs a receptive-field basis function. The number of blocks $n_B$ is greater than two and the number of components in the association memory space is $n_A = n \times n_B$. For given $i^{th}$ input $c_{ri}$ with the mean $m_{ij}$ and variance $\sigma_{ij}$, we adopt Gaussian function as the receptive-field basis function $\phi_{ij}$ for $j_{th}$ block, which can be defined as:

$$\phi_{ij} = exp[\frac{-(c_i - m_{ij})^2}{\sigma_{ij}^2}] \quad j = 1, 2, ..., n_B \tag{1}$$

where $\phi_{ij}(k-1)$ denotes the value of $\phi_{ij}(k)$ trough a time delay.

(3) Receptive-field space F: Areas formed by blocks are defined as receptive-fields. The number of receptive-fields is $n_R$, which equals $n_B$. The $j_{th}$ multi-dimensional receptive-field function is represented as

$$b_j(c, m_j, \sigma_j) = \prod_{i=1}^{n} \phi_{ij} = exp[-(\sum_{i=1}^{n} \frac{(c_i - m_{ij})^2}{\sigma_{ij}^2})] \tag{2}$$

where $m_j = [m_{1j}, m_{2j}, ..., m_{nj}]^T \in R^n$ and $\sigma_j = [\sigma_{1j}, \sigma_{2j}, ..., \sigma_{nj}]^T \in R^n$. The multi-dimensional receptive-field functions can be expressed in a vector form as

$$\Gamma(c, m, \sigma) = [b_{1j}, b_{2j}, ..., b_{nj}]^T \tag{3}$$

(4) Weight memory space W: Each location of F to a particular adjustable value in the weight memory space can be defined as

$$\mathbf{w} = [\mathbf{w}_1, \mathbf{w}_2, ..., \mathbf{w}_{nR}]^T = \begin{bmatrix} w_{11} & \cdots & w_{1p} \\ \vdots & \ddots & \vdots \\ w_{nR1} & \cdots & w_{nRp} \end{bmatrix} \tag{4}$$

where $w_j$ denotes the connecting weight value of the output associated with the $j_{th}$ multi-dimensional receptive-field. $p$ is the number of the output value.

(5) Output space Y: The output of RCMAC is the algebraic sum of the activated weights in the weight memory,

$$\mathbf{y} = [y_1, y_2, ..., y_{n_p}] = w^T \Gamma(c, m, \sigma) \tag{5}$$

## 3   Hand tracking

### 3.1   Orientation measurement

The FQA, which is based on Earth gravity and magnetic field measurements, is used to estimate the orientation of a rigid body [15]. But this algorithm is applied for static or slow-moving rigid body only. To make it applicable for relatively large linear accelerations, CMAC fusion algorithm is used together with angular rate information to estimate orientation of dynamic body (either slow-moving or fast-moving) in the next section. For the estimation of the orientation, the quaternion states and the angular velocities (measured by IMU) are used as input elements,

$$\mathbf{c}_{ori} = [q_0, q_1, q_2, q_3, w_x, w_y, w_z] \tag{6}$$

where $(w_x, w_y, w_z)$ is the vector of angular velocities. The input dimension $n_{ori}$ is seven.

The output vector is

$$y_{ori} = [q_0, q_1, q_2, q_3] \tag{7}$$

## 3.2  Hand position tracking

Since the human operator holds the IMU to measure the orientation of his hand, the position of the IMU is equal to the position of the human hand. Moreover, the color of the IMU is special, so it is easier to be identified than the human hand. In the IMU position tracking system, we use a 3D camera to obtain two 2D images of the IMU: color image and depth image. The IMU positions are tracked through Camshift algorithm, which is more and more noticed by means of its favorable performance in reality and robust.
For the estimation of the position, we use the translation $p_x, p_y, p_z$ (measured by Kinect) and the acceleration $a_x, a_y, a_z$ (measured by IMU) as input elements,

$$\mathbf{c}_{pos} = [p_x, p_y, p_z, a_x, a_y, a_z] \tag{8}$$

The input dimension $n_p os$ is seven. The output vector is

$$y_{pos} = [p_x, p_y, p_z] \tag{9}$$

## 4  Adaptive Multispace Transformation (AMT)

Robot manipulator has inherent perceptive limitations (such as perception of distance) and motor limitations (such as physiological tremor), which prevents the operator from operating precisely and smoothly enough for certain tasks [16]. For improving the visual and motor performance of teleoperation interface, we applied the modified version of Adaptive Multi-space Transformation (AMT) [16]. In the proposed method, an interface which introduces two scaling processes link the human operator working space to the robot working space (Fig. 3). The first change scales the movement produced by the human operator. Another change of scale is applied between the virtual unit vector K of the central axis of the robot EE and the robot movements. Such changes of scale modify the robot speed and, thus, improve performance.

The scaling vector $S$ is used to relate the actions of the human hand in master space MS and the movement of the virtual unit vector $K$ in the visual space VS. Another scaling variable $u$ is used to relate the VS space to the robot working space WS. $S$ and $u$ are a function of the distance $r$ between robot EE and the target. When $S < 1$, it decelerates the movement of $K$. Instead, it accelerates the movement of $K$ while $S > 1$.
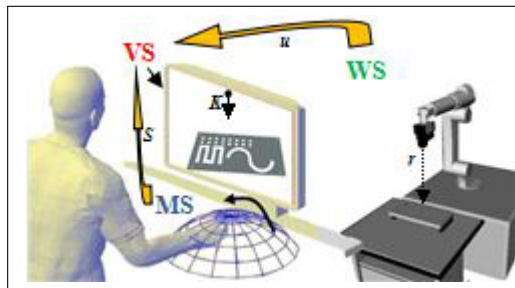


Figure 3: Representation of the human-interface-robot spaces

As the movement of the virtual position in VS is affected by vector $S$, let $S = [S_{pos}, S_{ori}]$, where $S_{pos}$ is the scaling vector of the position and $S_{ori}$ is the scaling variable of the orientation.

The Euler angular velocity in MS is $\dot{o_M}$ and $\dot{o_y}$ is the angular velocity in VS. Then

$$\dot{o_V} = \begin{cases} S_{ori}\dot{O_M} & \dot{O_M} \le \delta_{ori} \\ 0 & \dot{O_M} > \delta_{ori} \end{cases} \tag{10}$$

where $\delta_{ori}$ is the threshold value. Assume that $\dot{P_M}$ is the velocity vector of hand movement in MS and $\dot{P_V}$ is the speed of the vector $K$ in VS, the mapping vector of $\dot{P_M}$ in the VS is $\dot{P_M}'$. Let $S_{pos} = [s_K s_{K_\perp}]$ and $K_\perp$ is a vector which is perpendicular to $K$. In addition, $K_\perp$, $K$ and $\dot{P_M}$ are coplanar. So we have

$$\begin{aligned} p_K &= \begin{cases} S_K \bullet (|\dot{P_M'}| \bullet cos\theta) \bullet K = s_K \bullet K \bullet P_{M'} \bullet K & S_K \le \delta_K \\ 0 & S_K > \delta_K \end{cases} \\ P_{K_\perp} &= \begin{cases} S_{K_\perp} \bullet (|\dot{P_M'}| \bullet sin\theta) \bullet K_\perp = s_{K_\perp} \bullet K_\perp \bullet P_{M'} \bullet K_\perp & S_K \le \delta_K \\ 0 & S_{K_\perp} > \delta_{K_\perp} \end{cases} \end{aligned} \tag{11}$$

where $\delta_K$ and $\delta_{K_\perp}$ are the threshold value. Then the speed $\dot{P_V}$ of the vector $K$ is given as

$$\dot{P_V} = p_K + p_{K_\perp} \tag{12}$$

When $s_K = s_{K_\perp}$, the speed $\dot{p_V}$ results in $\dot{P_V} = s_K P_{M'}$. While $s_K < s_{K_\perp}$, it requires greater precision in the direction of the central axis of EE. Instead, the direction which is perpendicular to the central axis requires greater precision with $s_K > s_{K_\perp}$. In this paper, we use $s_K > s_{K_\perp}$ so that the operator can easy to center the axis of the hole, as well as insert the peg into the hole quickly. Since $S_{ori}$ and are functions of distance $r$, the function $S_{ori}(r)$ is defined as

$$\begin{cases} S_{ori}(r) = log(r) + C_1 \\ S_{K_\perp}(r) = log(r) + C_2 \\ S_K(r) = \sqrt{r} + C_3 \end{cases} \tag{13}$$

where $C_1$, $C_2$ and $C_3$ are constants.

## 5 Experiments

### 5.1 Environment of experiment

A comparison experiment was designed to verify the proposed method. In the experiment, a series of screwing bolt tests were carried out to compare our method with methods [11, 12] in efficiency of the manipulation. The three methods controlled the position and orientation of robot EE directly to screw the bolt into the nut. Joint angles can be achieved by the solution of robot inverse kinematics. Given a posture of robot EE, the angle of each joint can be achieved by the robot inverse kinematics [17]. Fig. 4 shows the environment of the experiment.
Two GOOGOL GRB3016 robots were used in our experiments. Tab. 1 lists the nominal robot link parameters of the robot. Two robot manipulators were placed at the distance of 205.3 cm. The operator stood in the front of the Kinect and held an IMU. The leap motion sampled at 30 HZ. The diameter of the nut was 75.5 mm and the diameter of the bolt was 75 mm (Fig. 5). The length of the nut was 91 mm and that of bolt was 83 mm. In each task, the operator needed to control the robots and screwed the bolt into the nut.

Figure 4: Environment of experiment

Table 1: The DH parameters for the GOOGOL GRB3016 robot(a: link length.: link twist. d: link offset.: joint angle.)

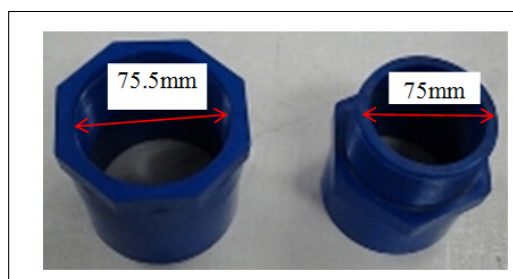| JointDH | a(mm) | $\alpha$ (rad) | d (mm) | $\theta$ (rad) |
|---------|-------|----------------|--------|----------------|
| 1 | 150 | $-\pi/2$ | 250 | 0 |
| 2 | 570 | $-\pi$ | 0 | $-\pi/2$ |
| 3 | 150 | $\pi/2$ | 0 | 0 |
| 4 | 0 | $-\pi/2$ | 650 | 0 |
| 5 | 0 | $-\pi/2$ | 0 | $-\pi/2$ |
| 6 | 0 | 0 | -200 | 0 |



Figure 5: The screw nut and the screw bolt

## 5.2     Results of experiment

In the proposed algorithm, CMAC was used to estimate the orientation and the position of the human hand. Fig. 6 shows the 3-D path of two robot end-effectors during the screwing bolt experiment. The whole time of each test was about 240s. Fig. 7 shows the results of tracking the robot EE in the period of adjusting the position and orientation (about 35 s). The period of screwing blot was ignored since the position and the orientation did not change greatly. Fig. 7 (a, b, c) shows the position in X, Y, Z and Fig. 7 (d, e, f) shows the orientation in Yaw, Pitch and Roll. The dotted lines are the measured data (ML) received from the left hand. The dash dot lines are the measured data (MR) received from the right hand. The star lines are the estimated data of the left robot EE (EL). The plus lines are the estimated data of the right robot EE (ER). The estimation algorithms could reduce the noise and improve the operating accuracy. Since the gap between the blot and the nut was 0.5 mm, whether the operator could screw the blot into the nut was used to evaluate the accuracy of the three methods. Moreover, we compared the efficiency between our method and methods [11, 12], including the operation time and times of faults in each test.
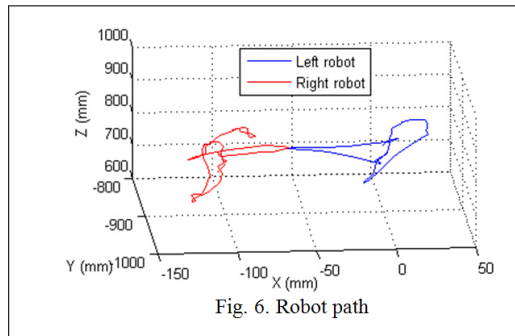

Fig. 6. Robot path

Figure 6: Robot path

The three methods were compared in terms of operation time and times of faults. The operation time includes closing the two robot end-effectors, adjusting the two robot end-effectors, screwing the bolt and separating the two robot end-effectors. The times of faults are the number of the operator tries to screw the bolt into the nut in each test. Tab. 2 shows the results of the operation time and times of faults for 5 tests, respectively. For test results of our method, the operation time for 5 tests ranges from 161 s to 169 s, with the mean time of 165.0 s. For methods [11, 12], the mean time is 193.4 s and 213.4 s. The mean times of faults are 3.6 and 5.6. Compared with methods [11, 12], the mean time of our method drops about 28.4 s and 48.4 s. Moreover, the times of faults of our method drops about 2.19 and 4.19.

Table 2: The DH parameters for the GOOGOL GRB3016 robot(a: link length.: link twist. d: link offset.: joint angle.)

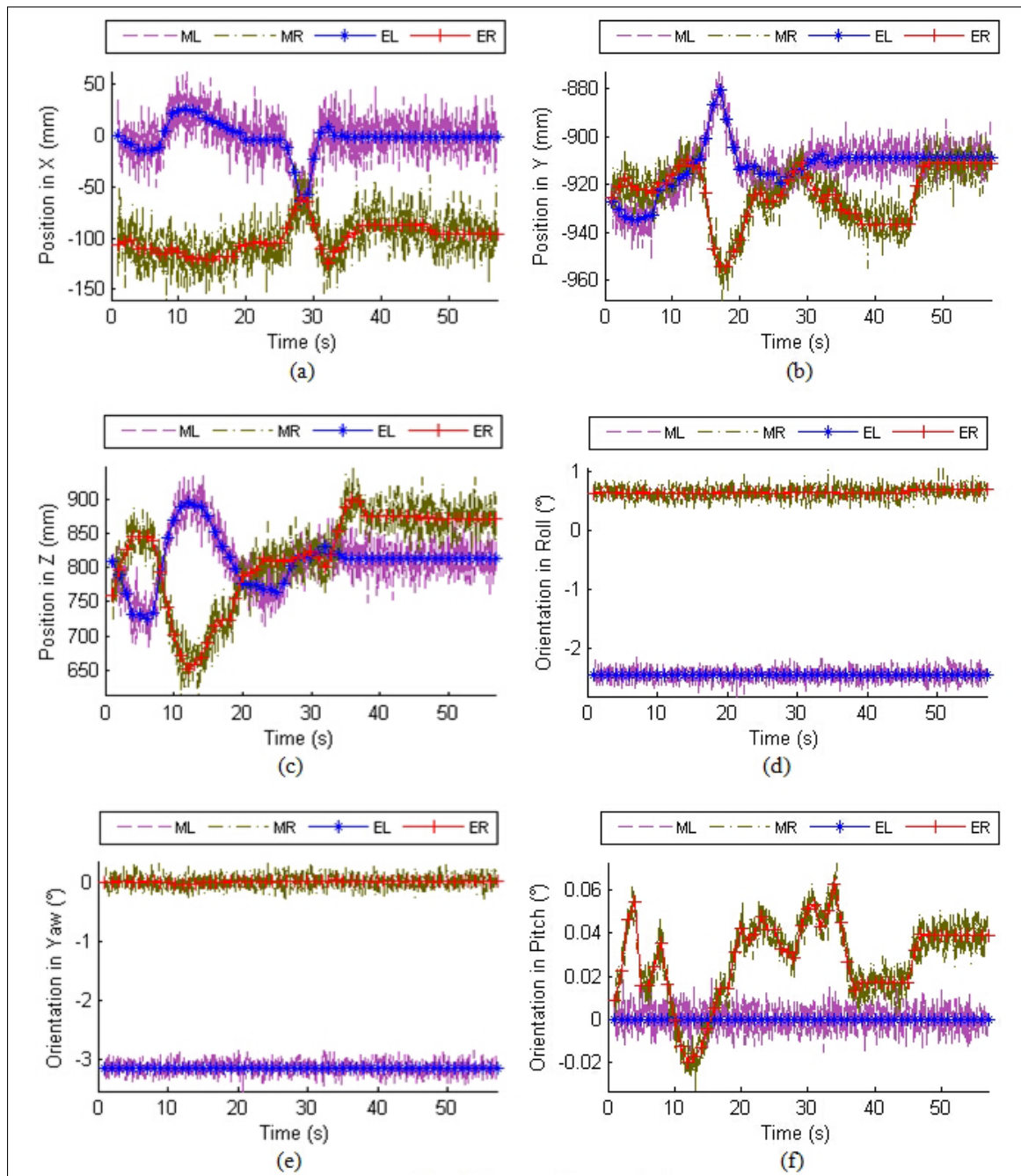|  |  | 1 | 2 | 3 | 4 | 5 | Mean |
|---|---|---|---|---|---|---|---|
| Our method | Time / s | 165 | 161 | 166 | 169 | 164 | 165.0 |
|  | Times | 2 | 2 | 1 | 1 | 1 | 1.41 |
| Method [11] | Time / s | 191 | 188 | 194 | 198 | 196 | 193.4 |
|  | Times | 4 | 3 | 3 | 5 | 3 | 3.6 |
| Method [12] | Time / s | 211 | 208 | 214 | 218 | 216 | 213.4 |
|  | Times | 6 | 5 | 5 | 7 | 5 | 5.6 |

Figure 7: Peg tracking results

# 6    Discussions

This paper proposes a robot control method based on hybrid sensors. The motions of robot manipulators are controlled by imitating the motions of operators. For the robot teleoperation in the remote unstructured environment, a condition is assumed that all the remote robot site components can be installed on a mobile platform and enters those unstructured environment. And the remote unstructured environments involve robotic arm, robot controller, cameras on end-effectors, and some other cameras. The method shown here was testified by screwing a bolt into a nut. This system includes the operator into the decision control loop and that is a significant advantage. Firstly, it allows a robot to finish some tasks like moving without any prior knowledge like start location and even destination location. Secondly, there are some similar tasks requiring decision making. When picking objects or cleaning some objects which may contain some dangerous items, decision making is always required. Also it is expected that this system can be used to achieve the complex postures when the joints of the robot are limited. Compared with contacting electromagnetic devices, like hand joystick and data gloves, our method would not hinder most natural human-limb motion and allows the operator concentrate on his own task instead of decomposing commands into some simple operations. Compared with the non-contacting markerless method [11, 12], our method was proved more accurate and efficient. Moreover, as the manipulation task to be more complex, multiple robot cooperation will become a trend. However, the contacting interfaces used in teleoperation for the multiple robot manipulators often require multiple operators [18]. In this paper, it only needs one operator to control two robot-manipulators to complete complex manipulation.

In the future, gesture control will be combined with voice control. Simple commands like start, end, and pause can be completed by voice. Then the system will work more flexibly and advantageously.

# 7    Conclusions

This paper presents a human-robot interface system which uses a tracking technology based on hybrid sensors. To eliminate the effect of occlusion and failure of motion sensing, CMAC is developed to estimate the orientation and position information of the human hand. Since robot manipulator have inherent perceptive limitations and motor limitations, the high-precision tasks cannot be performed directly by the operator. Thus, AMT system is employed to assist the operator to complete the high-precision tasks.

In the experiment raised in this paper, screwing tasks have been carried out. We compared the efficiency between our method and method [11, 12]. Experimental results show that our method has better accuracy and efficiency. Further investigation of finger positioning will be considered to improve the performance of the human-robot interaction method.

# Bibliography

[1] T. Ando, R. Tsukahara, M. Seki (2012); A Hapic Interface Force Blinker 2 for Navigation of the Visually Impaired, *IEEE Trans. on Industrial Electronics*, 59(11): 4112-4119.

[2] K. Kiguchi, S. Kariya, K. Watanabe (2003); An exoskeletal robot for human elbow motion support-sensor fusion, adaptation, and control, *IEEE Trans. on Systems, Man, and Cybernetics, Part B: Cybernetics*, 31(3): 353-361.

[3] GL. Du, P. Zhang, LY. Yang, YB. Su (2010); Robot teleoperation using a vision-based manipulation method, *Audio Language and Image Processing*, (ICALIP 2010 Int. Conf., Shanghai, 945-949.

[4] A. Peer, H. Pongrac, M. Buss (2010); Influence of Varied Human Movement Control on Task Performance and Feeling of Telepresence, *Presence-Teleoperators and Virtual Environments*, 19(5):463-481.

[5] V. Siddharth (2004); *Vision-based markerless 3D human-arm tracking*, M.A.Sc. Thesis, Dept. of Mech. Eng., University of Ottawa, Canada.

[6] YH Ma, ZH Mao, W. Jia, C. Li, J. Yang, Magnetic Hand Tracking for Human-Computer Interface, *IEEE Trans. on Magnetics*, 47(5): 970-973, 2011.

[7] K.C.C. Peng, W. Singhose, D.H.Frakes (2012); Hand-Motion Crane Control Using Radio-Frequency Real-Time Location Systems, *IEEE Trans. on Mechatronics*, 17(3): 464-471.

[8] M. Khezri, M. Jahed (2011); A Neuro Fuzzy Inference System for sEMG-Based Identification of Hand Motion Commands, *IEEE Trans. on Industrial Electronics*, 58(5): 1952-1960.

[9] A.R.Varkonyi-Koczy, B.Tusor (2011); HumanComputer Interaction for Smart Environment Applications Using Fuzzy Hand Posture and Gesture Models, *IEEE Transactions on Instrumentation and Measurement*, 60(5):1505-1514.

[10] B. Ionescu, D. Coquin, P. Lambert, V. Buzuloiu (2005); Dynamichand gesture recognition using the skeleton of the hand, *Journal on Applied Signal Processing*, 2101-2109.

[11] GL Du, P Zhang (2014); Markerless Human-Robot Interface for Dual Robot Manipulators Using Kinect Sensor, *Robotics and Computer Integrated Manufacturing*, 30(2): 150-159.

[12] J. Kofman, S. Verma, X. Wu (2007); Robot-Manipulator Teleoperation by Markerless Vision-Based Hand-Arm Tracking, *Int. J. of Optomechatronics*, 1(3): 331-357.

[13] R. Marin, PJ. Sanz, R. Wirz (2005); A Multimodal Interface to Control a Robot Arm via the Web: A Case Study on Remote Programming, *IEEE Transactions on Industrial Electronics*, 52(6): 1506-1521.

[14] CM. Lin, LY. Chen, DS. Yeung (2010); Adaptive Filter Design Using Recurrent Cerebellar Model Articulation Controller, *IEEE Trans. on Neural Networks*, 19(7): 1149-1157.

[15] X. Yun, ER. Bachmann, RB. McGhee (2008): A Simplified Quaternion-Based Algorithm for Orientation Estimation From Earth Gravityand Magnetic Field Measurements, *IEEE Trans. on Instrumentation and Measurement*, 57(3): 638-650.

[16] LM. Munoz, A. Casals (2009); Improving the Human-Robot Interface Through Adaptive Multispace Transformation, *IEEE Trans. on Robotics*, 25(5): 1208-1213.

[17] G. Antonelli, S.Chiaverini, G. Fusco (2003); A new on-line algorithm for inverse kinematics of robot manipulators ensuring path tracking capability under joint limits, *IEEE Trans. on Robotics and Automation*, 19(1): 162-167.

[18] R. Marin, PJ. Sanz, R.Wirz (2005); A Multimodal Interface to Control a Robot Arm via the Web: A Case Study on Remote Programming, *IEEE Trans. on Industrial Electronics*, 52(6): 1506-1521.